Application of Variational Monte Carlo methods on confined electrons

Bror Hjemgaard, Carl Martin Fevang, Håkon Kvernmoen

December 19, 2020

Abstract

Using the Variational Monte Carlo (VMC) method we estimated the ground state energy of two 3D quantum dots electrons in a harmonic oscillator potential. The study was broken down into a variational study of two systems; one where the electric interactions of the electrons was ignored, and one where it was accounted for, through the parameters α and β. Aiming for a metropolis acceptance rate of 50%, the required step size, δ' was found to be $\delta \approx 1.389/\sqrt{\alpha\omega}$. The systems stabilized after 10^5 Monte Carlo cycles. The variatioal method on a 3D harmonic oscillator yielded the lowest energy state for $\alpha = 1$ at 3ω, coinciding with theory. Optimized parameters, $\alpha = 0.88$ and $\alpha = 0.994, \beta = 0.286$, respectively, for two trial functions yielded the ground state energies of 3.77 a.u and 3.73 a.u. The pure harmonic oscillator was found to perfectly fit the virial theorem, while a superimposed Coulomb potential only fit under certain conditions.

1 Introduction

In the futile debate over which elementary particle is most important, the electron has a strong case. Electrons are central to so many of the modern technologies we develop, from anything to do with power, to the material properties of many of the most useful, and exotic, materials to come from nanotechnology. A particularly hot study in the aforementioned field of nanotechnology is the quantum dot; a semiconducting, quantum mechanical material comprised of electrons confined in in atom-like structures. These quantum dots have applications within LED-lasers, single-electron transistors, solar cells, quantum computing, cell biology and the list goes on. We will in this paper study as simple model of a quantum dot with two electrons trapped in a harmonic oscillator potential.

The electron is however a mildly cumbersome particle, seeing as it interacts with the electromagnetic field. This gives rise to Coulomb interaction between electrons that make the quantum mechanical properties of systems containing multiple electrons non-trivial to derive. We will specifically study the ground state energy of a quantum dot with two electrons; the simplest case of multiple electrons. However, our methods shall be a proof of concept for methods that can be generalized to any number of interacting particles.

Using the variational method with two different types of trial wave functions for the ground state of the system, we seek insight into its properties. This gives rise to multidimensional integrals, where we will apply Monte Carlo methods, and the Metropolis algorithm, to hopefully get good numerical results.

We will compare these results with results from an earlier study of this system, that time using Jacobi's method of finding eigenvalues for a simplified version of the system.[1] Lastly, we will see how our results stack up with the virial theorem, and see whether this can give us any further insight the properties of the system.

[1] C. M. Fevang and H. Kvernmoen. "Implementation of the Jacobi eigenvalue method with classical and quantum mechanical applications". In: (Sept. 2020). URL: https://github.com/hkve/FYS3150/blob/master/Project2/report/Project2_final.pdf.

2 Theory

Throughout this paper, we will be using natural units. In particular this means energy will given in atomic units (a.u.) and distances will be unitless. For information see Appendix A.

2.1 Quantum dot model

The system we will be scrutinizing in this report is a model of a *quantum dot*. These are systems where a number of electrons are trapped in a potential well of sorts. Modelling it with a harmonic oscillator potential, and letting there be N particles entrapped, the Hamiltonian can written

$$\hat{H}_0 = \sum_{i=1}^{N} -\frac{1}{2}\nabla_i^2 + \frac{1}{2}\omega^2 r_i^2 \tag{1}$$

where we label the positions of the individual particles $\mathbf{r}_i$ [2], and the Laplacian operating on particle i is labeled ∇_i^2. ω is the characteristic frequency of the oscillator potential.
We will study a quantum dot where there are electrons trapped in the potential, which will add a Coulomb interaction between the electrons. This Coulomb interaction adds terms to the Hamiltonian system according to

$$\hat{H}_1 = \sum_{i}^{N}\sum_{j\neq i}\frac{1}{2}\frac{1}{r_{ij}} = \sum_{i}^{N}\sum_{j<i}\frac{1}{r_{ij}}, \tag{2}$$

where $r_{ij} = |\mathbf{r}_i - \mathbf{r}_j|$, and we make use of the fact that $r_{ji} = r_{ij}$.
For two electrons, the complete Hamiltonian, including the Coulomb interaction, becomes

$$\hat{H} = -\frac{1}{2}\left(\nabla_1^2 + \nabla_2^2\right) + \frac{1}{2}\omega^2\left(r_1^2 + r_2^2\right) + \frac{1}{r_{12}} \tag{3}$$

2.2 Trial wave functions

We will study the quantum dot system for two electrons, exploring the ground state energy of the system using the *variational method* described in Appendix B. We will study two types of trial wave functions. The first of these will have a single parameter, and is Gaussian function centered on 0:

$$\Psi_{T1}\left(\mathbf{r}_1, \mathbf{r}_2\right) = C\exp\left(-\alpha\omega\left(r_1^2 + r_2^2\right)/2\right). \tag{4}$$

Here the variational parameter is α, which will dictate how narrow the probability distributions of the electrons are.
The second trial wave function class build on the first one, adding a second term which accounts for a repulsion between the electrons:

$$\Psi_{T2}\left(\mathbf{r}_1, \mathbf{r}_2\right) = \Psi_{T1}\left(\mathbf{r}_1, \mathbf{r}_2\right)\cdot\exp\left(\frac{r_{12}}{2\left(1+\beta r_{12}\right)}\right) \tag{5}$$

The added variational parameter β dictates the bias of the probability distribution for configurations where the electrons are apart from each other.
The trial wave functions are described in more detail in Appendix C. The *local energy*[3] of the first trial wave function is

$$E_{L1} = \frac{1}{2}\omega^2\left(r_1^2 + r_2^2\right)\left(1-\alpha^2\right) + 3\alpha\omega \tag{6}$$

when ignoring the Coulomb interaction, and

$$E_{L1} = \frac{1}{2}\omega^2\left(r_1^2 + r_2^2\right)\left(1-\alpha^2\right) + 3\alpha\omega + \frac{1}{r_{12}} \tag{7}$$

when taking the Coulomb interaction into account.
For the second wave function, the local energy is shown to be

$$E_{L2} = E_{L1} + \frac{1}{2(1+\beta r_{12})^2}\Bigg(\alpha\omega r_{12} - \frac{1}{2(1+\beta r_{12})^2} - \frac{2}{r_{12}} + \frac{2\beta}{1+\beta r_{12}}\Bigg). \tag{8}$$

2.3 Virial theorem

The **virial theorem** relates the average kinetic energy, $\langle T\rangle$, to the average potential energy, $\langle V\rangle$, of certain mechanical systems. Classically, if a conservative force between two particles, separated by a

[2] We will use the notation $r = |\mathbf{r}|$ to denote the magnitude of a vector $\mathbf{r}$.

[3] This quantity will be described in greater detail later, in section 2.4.

distance r, originates from a potential $V_n(r) \propto r^n$ for some n, then the virial theorem takes the simple form[4]

$$2\langle T\rangle = n\langle V\rangle, \tag{9}$$

where $\langle V\rangle$ represents the average *total* potential energy of the system.

2.4 Probability distribution

Some useful definitions of probability distributions from wave functions will be necessary. We define $\mathbf{R} = (\mathbf{r}_1, \mathbf{r}_2, ...\mathbf{r}_N)$, holding all spatial degrees of freedom of a system of N particles. Using the equation for the expectation value of the energy associated with a wave function $\Psi_T(\mathbf{R})$ from Appendix B equation (14), we can multiply the integrand by $\Psi_T(R)/\Psi_T(R)$ from the left, and add the integral in the denominator to take into account unnormalized states to get

$$\langle E\rangle = \frac{\int |\Psi_T(\mathbf{R})|^2 \frac{H(\mathbf{R})\Psi_T(\mathbf{R})}{\Psi_T(\mathbf{R})} d\mathbf{R}}{\int |\Psi_T(\mathbf{R})|^2 d\mathbf{R}}.$$

We now define our quantal probability distribution

$$P(\mathbf{R}) = \frac{|\Psi_T(\mathbf{R})|^2}{\int |\Psi_T(\mathbf{R})|^2}, \tag{10}$$

and a new property called the local energy, E_L, that has to be found analytically for each trial wave function:

$$E_L(\mathbf{R}) = \frac{H(\mathbf{R})\Psi_T(\mathbf{R})}{\Psi_T(\mathbf{R})}. \tag{11}$$

If the trial wave function is an eigenstate of the Hamiltonian, this quantity is constant. For more complicated systems, we normally don't have an eigenstate of the Hamiltonian and the local energy will not be constant. Therefore studying the variance in the local energy serves as a good metric for determining the correctness of our trial wave function.

[4] George Collins. *The virial theorem in stellar astrophysics*. Tucson: Pachart Pub. House, 1978. ISBN: 9780912918136.

Combing the probability distribution from equation (10) and the local energy from equation (11) we can write the expectation value for the energy as:

$$\langle H\rangle = \int P(\mathbf{R}) E_L(\mathbf{R}) d\mathbf{R}$$

Since the probability density function in equation (10) is the *ratio* between the absolute square of the wave function, we avoid the need for normalization. This is extremely beneficial as normalization would require an integral over the 6-dimensional solution space, which is very computationally expensive as discussed in the next paragraph.

3 Implementation

The code for the variational Monte Carlo method is written in `C++`. Plotting and data analysis is done in `Python`. All the code for simulations and plotting, as well as how to use it, is openly available at https://github.com/hkve/FYS3150/tree/master/Project5.

To implement the variational method we have to integrate over the 6-dimensional solution space. Due to the high number of dimensions, non-stochastic integration schemes becomes infeasible. As the absolute square of the wave function represents the probability density of the positions of the two electrons, most of the wave function will be close to zero and yield no contribution to the expectation values. By using the Monte Carlo based Metropolis algorithm we can sample points wherein the wave function is non-zero in order to avoid integrating over every point in the 6-dimensional solution space. An overview of the Metropolis algorithm is presented here.[5]

[5] B Hjemgaard, H. Kvernmoen, and C. M. Fevang. "Estimating the critical temperature of a ferromagnetic material using the 2D Ising model". In: (Nov. 2020). URL: https://github.com/hkve/FYS3150/blob/master/Project4/report/Project4.pdf.

3.1 Metropolis implementation

We begin by choosing a step length δ, number of Monte Carlo cycles τ and variational parameters α, β. We define $\mathbf{v} = (v_1, v_2..., v_6)$ as 6 independent random numbers in the range $v_i \in [-0.5, 0.5]$. Thereafter we initialize $\mathbf{R} = \delta\mathbf{v}$ as our initial position. Now for each Monte Carlo cycle we preform.

1. Propose a trial position $\mathbf{R}' = \mathbf{R} + \delta\mathbf{v}$.
2. Calculate the ratio of the absolute square of the trial wave function $w = |\Psi_T(\mathbf{R}')|^2/|\Psi_T(\mathbf{R})|^2$
3. Pick a uniformly random number $s \in [0, 1]$. If $w \geq s$, accept the proposal and set $\mathbf{R} = \mathbf{R}'$. If not, reject the proposal; keeping the old value.
4. Update the expectation values

When $|\Psi_T|^2$ has a larger value for the trial step, this algorithm ensures that we will move towards the more interesting areas of the wave function. The condition $w \geq s$ gives us some fluctuations around the high probability density and we won't get stuck on the highest $|\Psi_T(\mathbf{R})|^2$.

3.2 Optimizing parameters

As the wave functions will be dependent on one or more parameters, it is necessary to find the optimal parameters that gives the lowest energy expectation value. We do not know what the expectation value for the energy is before we have preformed the metropolis algorithm and has to be calculated for every set of parameters. This is the tedious part of the VMC and scales poorly with more parameters.

3.3 Random numbers

To make random numbers we will use a pseudorandom number generator (PRNG). PRNG's are never truly random and have a period after which the numbers will repeat (for a given seed). For every Monte Carlo cycle we will require six random numbers for the trial position and one for the condition $w \geq s$. As we are dealing with a stochastic algorithm, repetition of random numbers is something we want to avoid. We have opted to use the 64-bit version of the Mersenne Twister generator `(mt19937_64)`, with a period of 2^{19937} numbers. Assuming an upper bound of $\tau = 10^8$ cycles, this PRNG will sufficiently provide us with enough numbers.

4 Method

4.1 Pure harmonic oscillator potential

We will begin by calculating the ground state energy for the harmonic oscillator potential, not taking the Coulomb interaction into account. The trial wave function is then given by equation (4) and the corresponding local energy by equation (6). For this potential we can find the analytical wave function, corresponding to $\alpha = 1$ in our trial wave function. This means that the local energy should be constant $E = 3$ a.u. with zero variance for this α, serving as an excellent benchmark for our algorithm. Since this is the parameter corresponding to the lowest energy, all other α values should produce larger energies. We will also study how many Monte Carlo cycles are required to reach stable expectation values and if an equilibration phase is required.

4.2 Optimizing step length

The proposed state in the Metropolis algorithm depends on the step size δ. Before committing to the most requiring of simulations, we should establish a system for determining what δ to use under different conditions. Within the Metropolis method the ratio of accepted states to the number of proposed states is known as the *acceptance rate*. If the acceptance rate is too low or too high, the exploration of state space will be slow. This exploration rate has been shown[6] to be optimized at a 50% acceptance rate. We will thus aim to model δ as a function of relevant parameters in order to achieve a constant 50% acceptance rate. A constant acceptance rate will remove a degree of freedom from the system, allowing us to limit our study to the relevant attributes only.
After finding a dependable model of δ, it will be used

[6] Matthew Foulkes et al. "Quantum Monte Carlo simulation of solids". In: *Reviews of Modern Physics* 73 (Feb. 2001). DOI: 10.1103/RevModPhys.73.33.

to dynamically determine the step size for any simulation.

4.3 Coulomb interaction

Extending our Hamilton to include Coulomb repulsion, we would expect higher energies as we are adding a factor of r_{12}^{-1}. Initially we will try using the same trial wave function as we did in the pure harmonic oscillator case (4), noting that we have to include the repulsion term in the local energy, given by (7).
The Coulomb potential is dependent on the distance between the two electrons, so it would natural to assume that the wave function would be dependent on r_{12}. To incorporate the physics of electron correlation we add a so-called Jastrow factor[7] to the pure harmonic oscillator trial wave function, presented in equation (5). The local energy is then given by equation (8). We now have to variational parameters α and β and a more careful approach will be required to minimize the energy. Since Ψ_{T2} takes the electron-electron repulsion into account as well as having another variational degree of freedom, we predict that this trial wave function will preform better than Ψ_{T1}. We will also compare our results with an eigenvalue approach to the same problem.[8]

4.4 Variational minimum

The trial wave functions are built in with variational parameters (α for Ψ_{T1}, α and β for Ψ_2). This is by design, as we want to find the values for these parameters which minimizes the energy expectation value. The first trial wave function Ψ_{T1} is only dependent on α. To find the optimal parameter, we simply calculate the energy for different α values and search for the the lowest energy. We also want to take the variance into account, as a low variance is desired.
On the other hand, the second trial wave function Ψ_{T2} is dependent on both α and β. To minimize the energy in terms of these two parameters, we have proposed two different procedures.

4.4.1 Brute force

This method is essentially the same as for Ψ_{T1}. By choosing a range of α and β values, we can calculate the expectation value for the energy at every point in the grid and plot $\langle E \rangle$ as a function of α and β. This will result in a 3D plot visually displaying which α/β pairs result in low energies. On the other hand, most of the points will not be close to the optimal values and we have to calculate a lot of unnecessary points. These calculations require parallelization to be completed in a reasonable amount of time and this was done using `OpenMP`.

4.4.2 Individual variation

To avoid calculating many unnecessary α/β pairs, we devised an algorithm that varies the parameters individually. Using the best α for Ψ_{T1}, we can calculate the energy for a range of β values. Thereafter we choose the β resulting in the lowest energy and vary α. This cycle repeats until we are fairly confident we have found the desired values. We also reduced the α/β interval slightly after each cycle, to increase resolution when we close in on the lowest energy.

5 Results

5.1 Stability

Firstly, in order to obtain the most accurate values, we must assert stability upon the system in terms of the number of Monte Carlo cycles τ. For a system without Coulomb interactions, the mean energy $\langle E \rangle$ as a function of τ as well as the variance is shown in Figure 1.1 and Figure 1.2 respectively. The figures illustrate that the energies begin to stabilize around $\tau \sim 10^3$, and remain effectively stable from $\tau \sim 10^5$. Whats more, for $\alpha = 1$, the energy is both at its lowest and most stable value: 3 a.u., confirming with the theoretical predictions. From the variance we observe that a decrease in α causes larger inaccuracies than

[7] N. Drummond, Mike Towler, and R. Needs. "Jastrow correlation factor for atoms, molecules, and solids". In: *Physical Review B* 70 (Feb. 2008). DOI: 10.1103/PhysRevB.70.235119.

[8] Fevang and Kvernmoen, "Implementation of the Jacobi eigenvalue method with classical and quantum mechanical applications".

increasing by the same amount, something which will be discussed later.
Similarly, when taking the Coulomb interactions into account, Figure 2.1 and Figure 2.2 were produced, illustrating that a value $\alpha < 1$ was more stable and yielded lower energies than any other. This too will later be discussed upon further. Here too the energies seem to begin to stabilize at around $\tau \sim 10^3$ and seem fully stable after $\tau \sim 10^5$. Thus, we will henceforth only solve systems with $\tau \geq 10^5$ in order to assure the highest accuracy.

5.2 Optimizing step length

With Monte Carlo moves determined by $\mathbf{R}' = \mathbf{R} + \delta\mathbf{v}$, we aim to choose δ in such a way that roughly 50% of all proposals are accepted. It was quickly observed that the acceptance rate varied with α; thus we calculated the acceptance rate for $\alpha \in [0.1, 2.5]$, $\delta \in [0.1, 5]$ and $\omega = 1$, shown in Figure 3.1. Extracting the points where the acceptance rate is 50% yielded Figure 3.2.
Labeling the step size which resulted in a 50% acceptance rate as δ', a function fit of the shape $\delta'(\alpha) = m\alpha^{-b}$ yielded $m = 1.389, b = 0.500$ allowing us to determine the optimal step size δ' for any α when $\omega = 1$.
However; we will later aim to solve the system for $\omega \neq 1$, and we thus also studied the ω dependence of $\delta'(\alpha, \omega) = m(\omega)\alpha^{-b(\omega)}$. Repeating the above procedure for $\omega = 0.01, 0.1, 0.25, 0.5, 0.75$ yielded Table 1, where it becomes clear that $b(\omega) = 0.5$ is constant. $m(\omega)$ is plotted in Figure 4. Resembling the shape of Figure 3.2, a similar fit to $m(\omega)$ yielded $m(\omega) = 1.389 \cdot \omega^{-0.5}$. Thus, the final shape of the step size yielding a 50% acceptance rate δ' became

$$\delta'(\alpha, \omega) = 1.389 \frac{1}{\sqrt{\alpha\omega}}. \tag{12}$$

5.3 Calculating the energy

5.3.1 First trial wave function Ψ_{T1}

Applying the above, we calculated the energy for several α, initially only for $\omega = 1$. Together with the variance, the energies of the interactive and non-interactive systems are shown in Figure 5.1 and Figure 5.2. The non-interactive system has ground state energy $E = 3$ a.u. for $\alpha = 1$, while the interacting system has it ground state $E = 3.77$ a.u. for $\alpha = 0.88$. Meanwhile, the minima in Figure 5.2 are located at $\sigma_E = 0$ a.u., $\alpha = 1$ and $\sigma_E = 0.260$ a.u., $\alpha = 0.88$ for the non-interactive and interactive systems respectively.
These ground state energies seem to coincide with those shown in Figure 1.1 and Figure 2.1.

5.3.2 Second trial wave function Ψ_{T2}

The brute force minimization of α and β is presented in figure 6. This data gave the minimum energy expectation value of $\langle E \rangle = 0.73$ a.u. using the optimal parameters $\alpha = 0.994 \pm 0.006$ and $\beta = 0.28 \pm 0.01$. The uncertainties used is the resolution of the grid. Preforming the individual variations, the energy again converged to 3.73 a.u. using the optimal parameters $\alpha = 0.994 \pm 0.001$ and $\beta = 0.286 \pm 0.005$. The uncertainties used is the resolution in the last variation iteration. These two sets of α and β values correspond within the uncertainties, and we chose to use the latter set due to having a lower uncertainty.

5.4 Comparison

Using the optimal parameters found, we can compare the energy expectation values for the two trial wave functions with the eigenvalue solver. This is resented in table 2. The second trial wave function Ψ_{T2} consistently produced lower values than Ψ_{T1} as predicted. Both wave functions results in higher energies than that of the eigenvalue solver.
A comparison of relative distance expectation values is presented in table 3. As the potential frequency increases, we see a decrease in the relative distance. The second trial wave function Ψ_{T2} consistently produced higher expectation values for the relative distance compared with Ψ_{T1}. When neglecting the Coulomb repulsion, the relative distance decreases for all ω compared with the Coulomb repulsion.

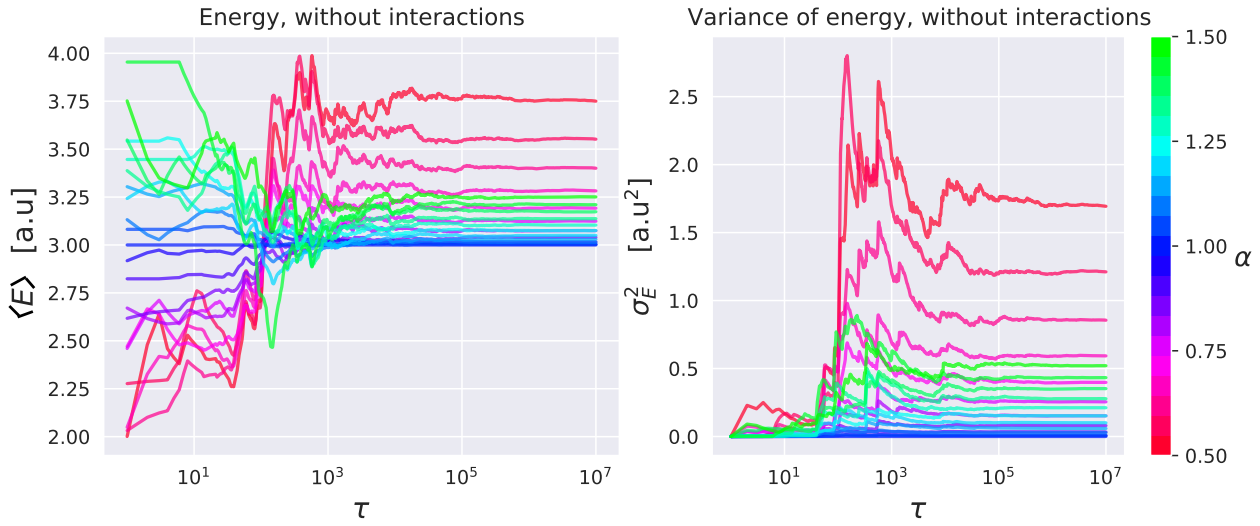

Left, Figure 1.1: $\langle E \rangle$ For system *without* interactions plotted against τ.
Right, Figure 1.2: Variance of energy of same interacting system plotted against τ.

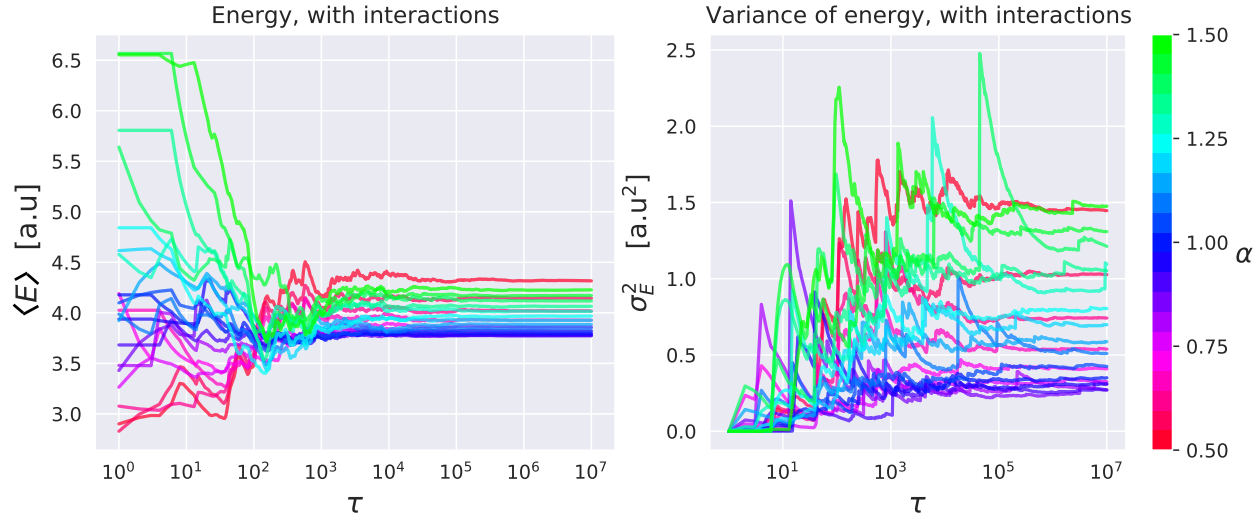

Left, Figure 2.1: $\langle E \rangle$ For system *with* interactions plotted against τ.
Right, Figure 2.2: Variance of energy of same interacting system plotted against τ.

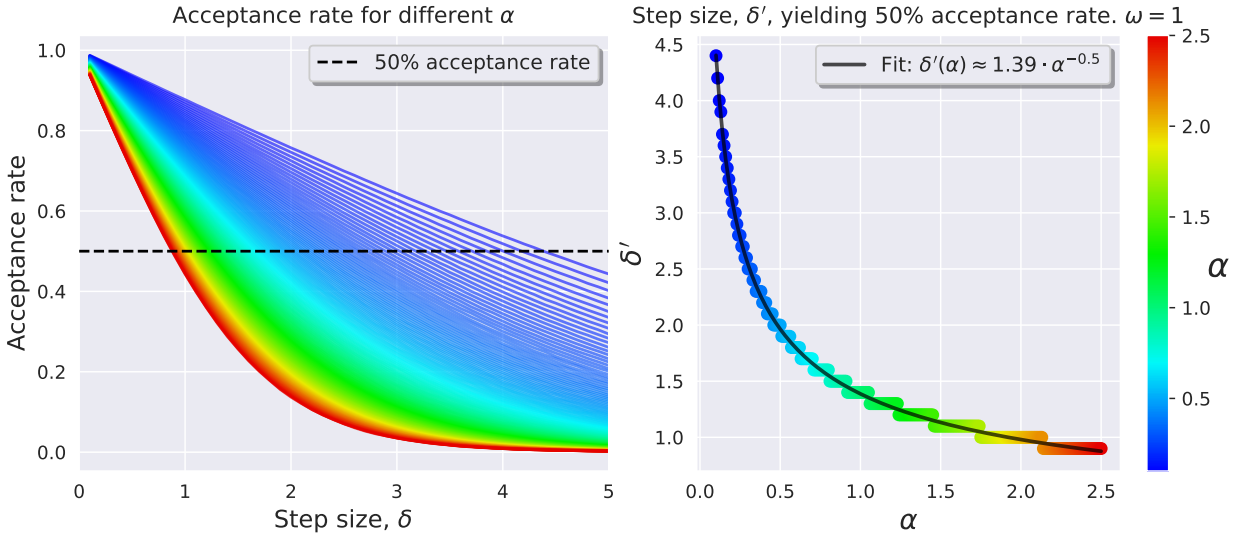

Left, Figure 3.1: Acceptance rate as a function of step size δ for several α and $\omega = 1$
Right, Figure 3.2: Step sizes yielding a 50% acceptance rate as a function of α

ω	$m(\omega)$	$b(\omega)$
0.01	13.9	0.498
0.1	4.39	0.501
0.25	2.77	0.500
0.5	1.96	0.500
0.75	1.60	0.500
1.0	1.39	0.500

Table 1: Fitted parameters m, b for a model $\delta'(\alpha) = m \cdot \alpha^{-b}$ at different ω. $\tau = 10^6$.

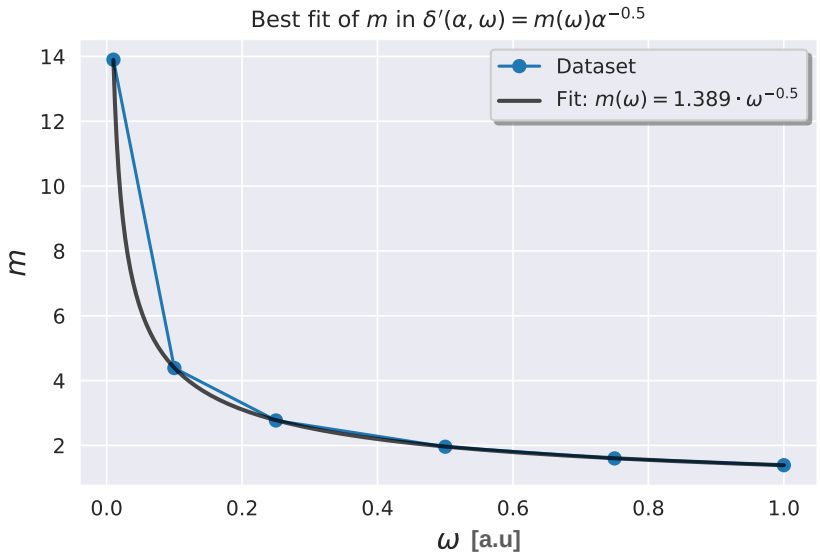

Figure 4: The fitted parameter m for different ω as well as a function fit of the shape $m(\omega) = c\omega^{-0.5}$

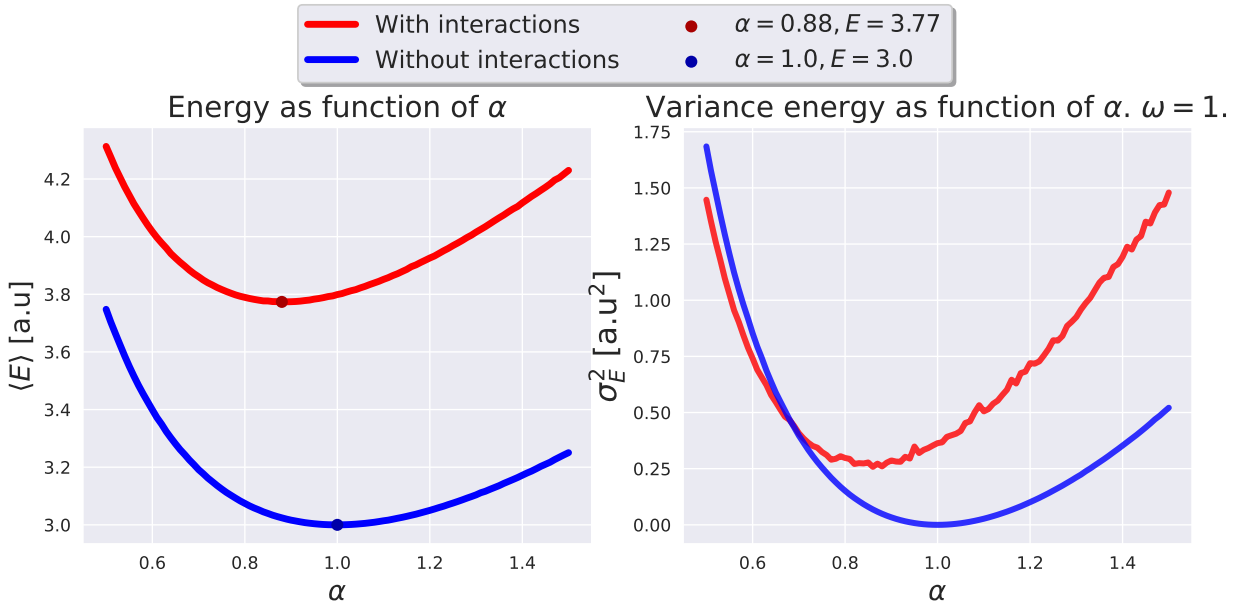

Left, Figure 5.1: $\langle E \rangle$ for both systems as functions of α. Minimums marked in legend. Right, Figure 5.2: Variance of energies of the same systems. $\omega = 1$ in both cases.

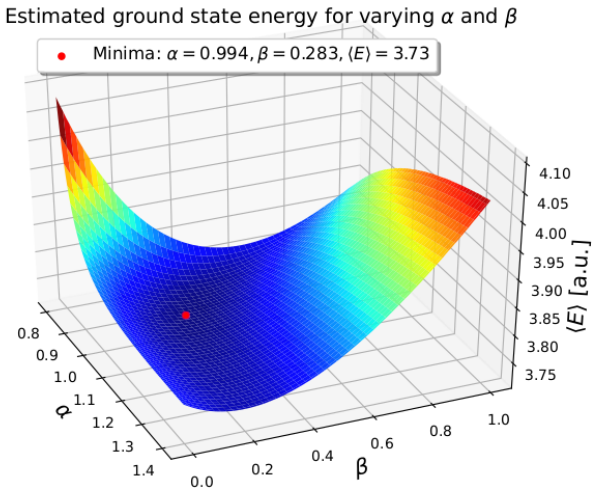

Figure 6: $\tau = 10^8, \omega = 1$ on the intervals $\alpha \in [0.8, 1.4]$ with a resolution $\Delta\alpha = 0.006$ and $\beta \in [0, 1]$ with a resolution $\Delta\beta = 0.01$. Ψ_{T2} was used with $\omega = 1$

ω	$\langle E \rangle \Psi_{T1}$	$\langle E \rangle \Psi_{T2}$	E_0
0.01	0.105	0.098	0.072
0.5	2.04	2.00	1.91
1	3.77	3.73	3.53
5	16.78	16.72	15.98

Table 2: Expectation values for energy from Ψ_{T1}, Ψ_{T2} and the eigenvalue solver E_0 for different frequencies. All results is presented in units of a.u. and calculations was done using $\tau = 10^8$ cycles.

5.5 Virial theorem

By the quantum mechanical Hamiltonian, the average kinetic energy is $\langle T \rangle = \langle E \rangle - \langle V \rangle$. After calculating the mean potential and kinetic energies, the *virial ratio* $\langle T \rangle / \langle V \rangle$ of both systems was plotted as functions of ω in Figure 7. The non-interactive system had a constant ratio while the interactive system had a lower ratio, approaching the non-interactive system from beneath.

ω	$\langle r_{12}\rangle$ HO	$\langle r_{12}\rangle$ Ψ_{T1}	$\langle r_{12}\rangle$ Ψ_{T2}
0.01	15.95	16.82	17.57
0.5	2.26	2.38	2.59
1	1.60	1.68	1.81
5	0.71	0.75	0.78

Table 3: Expectation values for the relative distance from Ψ_{T1} and Ψ_{T2} for different frequencies. The first column is the pure harmonic oscillator potential with no Coulomb repulsion (done with Ψ_{T1}), while the two last columns include the Coulomb repulsion. All calculations was done using $\tau = 10^8$ cycles.

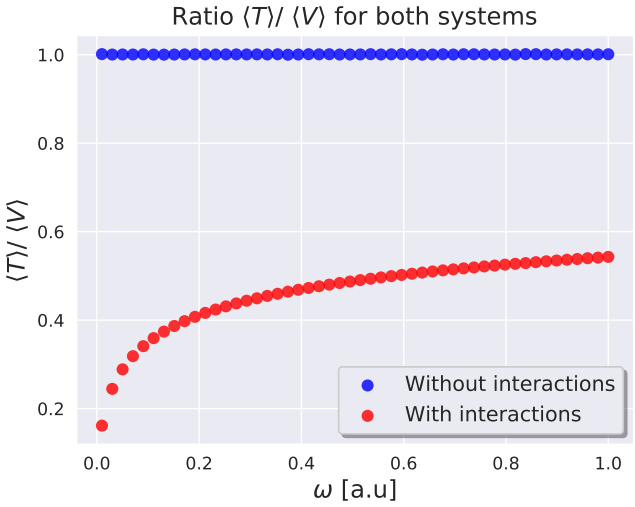

Figure 7: Computing the virial relation $\langle T\rangle/\langle V\rangle$ for both systems.

6 Discussion

6.1 Stability

Figure 1 illustrates that, in the non-interactive case, $\alpha = 1$ yields lowest and most stable energy, being stable for all τ. Its convergent value is 3 a.u. in accordance with the analytical prediction. In the case of $\alpha \neq 1$, however, the energies converge to values > 3 a.u., also with a higher variance, see Figure 1.2. An interesting question is as to why $\alpha < 1$ yield larger change in variance than $\alpha > 1$ does? The reasoning may be gotten from the fact that our wave function is Gaussian, meaning it has a well defined *full width at half maximum* (essentially a measure of the width of the curve):

$$\text{FWHM} = 2\sqrt{2\ln 2}\frac{1}{\sqrt{\alpha\omega}}. \tag{13}$$

Thus a *lower* α gives a *wider* distribution, meaning there are more r_1 and r_2, and thus more energies, to chose from, consequently giving a higher variance. That begs the question as to why $\alpha \to \infty$ does not converge upon the correct energy? The reason is because, as α increases and the FWHM decreases, the curve will eventually become so sharp that it start *excluding* the correct values, eventually diverging from the correct energy. This process is of course slower than the above, giving $\alpha > 1$ a higher variance than $\alpha < 1$. The idea is to find the sweet spot, which in this case is $\alpha = 1$.

Figure 2 has much of the similar qualities to Figure 1, the main difference being that an $\alpha < 1$ yields the lowest energy. We will soon discuss the reasoning behind this, but first we will address the fact that $\alpha > 1$ diverges at a similar rate to $\alpha < 1$, contrary to the non-interactive case discussed above. This attribute may once again be understood from the FWHM, this time keeping in mind the extra $1/r_{12}$ term added to the energy in (7). High $\alpha \to$ sharp distribution, and because the distribution is centered on 0, small r_{12} are extracted. Thus, at higher α, r_{12} of different (negative) orders of magnitude have roughly the same chance of being selected, while yielding *very* different energies due to the inverse proportionality.

That being said, there is a reason as to why the ground-state α is lower in the interactive case than in the non-interactive case. The two potentials may be, superficially, described as follows: the Coulomb potential pushes the particles away from each other, whilst the harmonic oscillator pulls them towards a common point. Thus, activating the electric potential should increase the distance between the particles, broadening the width of the distribution. From (13) we know that *decreasing* α has the same effect as broadening the distribution, explaining why the ground state of the interactive system has $\alpha < 1$. This result is in accordance with the minima of the

parabolas in Figure 5.1.

6.2 Optimizing step length

Our thorough study of the step length yielded a comprehensive model (12). Remembering that varying α is effectively the same as changing the frequency of the system, ω, it is reassuring that δ' is dependent of α and ω in the same inverse-root manner.
From (12) an interesting observation can be made. The parameter 1.389 closely resembles $2\ln 2 \approx 1.386$, meaning there are resemblance between δ' and the FWHM, (13). Assuming the above resemblance to be absolute, some quick algebra lets us postulate a relation between δ' and the FWHM:

$$\delta' = \sqrt{\frac{1}{2}\ln 2} \cdot \text{FWHM}.$$

While this is purely based on observations, it is noteworthy and deserving of further study in order to unveil the full relation. If one were to expand upon this relation the first step would of course be to compare the coefficient in (12) to $2\ln 2$ with an accuracy of more than 3 digits. Thereafter study the step size for other acceptance rates and relate them to the FWHM. This is, unfortunately, outside the scope of this report and not especially applicable to our problem. It is not unreasonable to guess a proportionality $\delta' \propto$ FWHM at any acceptance rate, not just at 50%, which neatly coincides with our above results. A more narrow distribution yields more similar extracted energies, which requires a smaller step length to differentiate them.

6.3 Variational minimum

Applying two methods two find the variational minimum for Ψ_{T2} resulted in equal values, reassuring us that we have actually found the optimal α and β. A more elegant solution would have been to calculate the gradient of $\langle E \rangle$ with respect to α and β and apply a iterative gradient descent method. Unfortunately time constraints made this infeasible to implement.

6.4 Calculating the energy

Looking back at table 2 we see that both Ψ_{T1} and Ψ_{T2} produce a higher energy than the values from the eigenvalue solver. This is reassuring, as the eigenvalue solver aims to solve the problem through the Schrödinger equation. How far off these values are from the analytical values would be speculation, but the results might be both larger or smaller than the true values. The values from the variational method on the other hand, must always be larger as shown in B. In addition Ψ_{T2} produced lower energies than that of Ψ_{T1}. This was expected as Ψ_{T2} has more variational degrees of freedom as well as incorporating r_{12} into its wave function. In addition the local energy for Ψ_{T1} in the interactive case does not fulfill the cusp-condition and will produce less credible values when r_{12} is very small (note the singularity in equation (18)).
Further in table 3 we see that the pure harmonic oscillator potential has a smaller $\langle r_{12} \rangle$ than the interactive case. This is due to the two electrons not interacting and there is no measure to pull them apart. For higher frequencies this difference becomes less notable. This is due to the harmonic oscillator potential overcoming the electron-electron repulsion. Presumably for very high frequencies these values would approximately be the same.

6.5 Virial theorem

By the proportionality to r^2 within the harmonic oscillator potential, the virial theorem (9) predicts $2\langle T \rangle = 2\langle V \rangle \Rightarrow \langle T \rangle / \langle V \rangle = 1$. This constant ratio is shown in Figure 7 for the non-interactive system.
However, for the interactive system in Figure 7, the ratio seems to stabilize as ω grows, and appears to diverge towards $-\infty$ as $\omega \to 0$. We may understand this behaviour by the following explanation: decreasing ω effectively "turns off" the harmonic oscillator, eventually leaving just the Coulomb potential. The virial theorem is only physically applicable when the relation $\langle T \rangle / \langle V \rangle$ is positive, i.e when the state is *bounded*. Our repelling Coulomb potential is most certainly not bounded, meaning the diverging behaviour in Figure 7 is reasonable. However, at

sufficiently large ω, the harmonic oscillator, which in of itself is a bounded potential, is strong enough to keep the repelling particles from fleeing to infinity, thus making the entire system bounded. This is expressed by the ratio $\langle T \rangle / \langle V \rangle$ being positive. As ω grows even further, the oscillator becomes the dominating potential, and it is thus reasonable to assume that the interactive-curve in Figure 7 eventually converges to $\langle T \rangle / \langle V \rangle = 1$ as $\omega \to \infty$.
The above logic implies that at some point the virial ratio of the interactive system crosses the x-axis and changes from an unbounded to a bounded system. Applying a function fit of shape $1 + a \cdot \omega^{-b}$ and solving for 0 revealed this point to be $\omega_0 \approx 0.004$.[9] At $\omega < \omega_0$ the state is unbounded as the particles escape of to infinity and the virial theorem does not apply (in a physical sense). At $\omega > \omega_0$ the state is bounded, forcing the particles into a attractive-repulsive mayhem.

7 Concluding remarks

We have successfully implemented the variational method using the the Monte Carlo based Metropolis algorithm. Starting off, we benchmarked our algorithm using the pure 3-dimensional harmonic oscillator. Using $\alpha = 1$ we achieved the analytical value of 3 a.u., with all other α values resulting in a greater energy. Investigating the stability of the algorithm we found that $\tau = 10^5$ cycles was sufficient to achieve stable expectation values. Trying to optimize the step length such that 50% of trial positions was accepted, we found that ideal step length followed $\delta' \approx 1.389/\sqrt{\alpha\omega}$.
Minimizing the energy in the interactive case, we found that $\alpha = 0.88$ was the optimal parameter for Ψ_{T1} and $\alpha = 0.994$, $\beta = 0.286$ for Ψ_{T2}. For $\omega = 1$ this resulted in an energy of 3.77 a.u. for Ψ_{T1} and 3.73 a.u. for Ψ_{T2}, where Ψ_{T2} resulted in energies closer to the results from the eigenvalue solver for all frequencies. This due to Ψ_{T2} incorporating more of the physical problem, as well as Ψ_{T1} not fulfilling the cusp-condition. With a increasing potential strength the expectation values for the realtive position decreased, with a larger energy.
Lastly we found that the pure harmonic oscillator potential resulted in equal kinetic and potential energy expectation values, in agreement with the virial theorem. Including the Coulomb repulsion we found that the ratio of kinetic and potential energy decreased as a function of ω, convergning to the pure harmoic oscillator when $\omega \to \infty$.

[9] This is not the most accurate of estimation as we are unsure of the actual function fit of the virial ratio. We may however assume that the order of magnitude is correct

8 Appendix

A Natural units

We apply natural units in this report, meaning the units will be defined in terms of physical constants. In particular we set the following constants equal to one.

$$\hbar = c = e = m_e = 1$$

Where $\hbar$ is the reduced Planck constant, c is the speed of light in vacuum, e is the elementary charge and m_e is the electron mass. This means that distances will be dimensionless and energy will be given in atomic units (a.u.). Doing this we makes equations prettier, effectively removing constants as well as scaling numbers to order of magnitude 1, minimizing roundoff errors.

B Variational method

Consider a Hermitian Hamiltonian operator $\hat{H}$ over a Hilbert space. The Hamiltonian must have a complete set $\{|\psi_n\rangle\}$ of eigenstates, where that $\hat{H}|\psi_n\rangle = E_n|\psi_n\rangle$. A set can be chosen such that the eigenstates are orthonormal, meaning the inner product of two eigenstates $\langle\psi_m|\psi_n\rangle$ becomes the Kronecker-delta function δ_{mn}. An arbitrary wave function ψ in the Hilbert space can then be written as a linear combination of the eigenstates of the Hamiltonian such that

$$|\psi\rangle = \sum_n c_n |\psi_n\rangle$$

where we assume a normalized state such that $\sum_n |c_n|^2 = 1$.
The *variational method* is based on this principle; letting E_0 denote the eigenvalue of the ground state $|\psi_0\rangle$, we can make an arbitrary *guess* for what the ground state can be, $\left|\tilde{\psi}_{GS}\right\rangle$. The expectation value of the energy of this trial state is guaranteed to overshoot the actual ground state energy; writing the state out as a linear combination described above, the expected energy of the state, $\tilde{E}_{GS}$, can be written as

$$\begin{aligned}
\tilde{E}_{GS} &= \left\langle \tilde{\psi}_{GS} \middle| \hat{H} \tilde{\psi}_{GS} \right\rangle \\
&= \sum_m \sum_n c_m^* \left\langle \psi_m \middle| \hat{H} c_n \psi_n \right\rangle \\
&= \sum_m \sum_n c_m^* c_n \langle \psi_m | E_n \psi_n \rangle \\
&= \sum_m \sum_n c_m^* c_n E_n \delta_{mn} \\
&= \sum_n |c_n|^2 E_n
\end{aligned}$$

Making use of the fact that the state is normalized, and that $E_n \geq E_0$ for all n, it follows that $\tilde{E}_{GS} \geq E_0$. This means we can safely make guesses for the wave function of the ground state, and know that the energy associated with such a wave function cannot be any lower than the actual ground state energy.
The variational method makes use of this, making a guess for the wave function $\tilde{\psi}$ of the ground state. However, the method is more powerful when a guess is not simply made for a single wave function, but for entire classes of wave function. These classes are made by creating wave functions that uses parameters that can be *varied*, as the name of the method implies. The trial wave function is then denoted $\psi(x; \alpha_1, \alpha_2, ...)$, where α_i are the *variational parameters*. Writing out the inner product above in the so-called position basis, we get an integral:

$$\tilde{E}_{GS} = \left\langle \tilde{\psi} \middle| \hat{H} \tilde{\psi} \right\rangle = \int_{-\infty}^{\infty} \tilde{\psi}^* \hat{H} \tilde{\psi} \, dx \tag{14}$$

Minimizing this integral with respect to the variational parameters will therefore give us the best approximation for the ground state wave function, within the class of functions spanned by $\{\tilde{\psi}\}$.

C Trial wave functions

We use two different classes of wave functions to apply when doing the Monte Carlo simulations to find the ground state energy of our system. When constructing these wave functions, some quantum mechanical considerations must be made. The wave

function of the system must take into account the quantum mechanical rules set for fermions, that they cannot occupy the same state. However, as we will simply look at a system of two electrons, we can let both electrons be in the same spatial state, assuming their spinors are opposite such that the total spin of the system is 0. We will thus make the assumption that the lowest energy state is symmetrical for both electrons, with total spin 0.

Treating the electron interaction as a perturbation to a pure quantum harmonic oscillator system, we will first try out a class of wave functions inspired by the ground state of this system. This ground state wave function is Gaussian[10] and it is therefore natural to try the class of Gaussian functions, the total wave function being the product of a Gaussian function for both electrons:

$$\Psi_{T1}(\mathbf{r}_1, \mathbf{r}_2) = Ce^{-\alpha\omega(r_1^2+r_2^2)/2} \tag{15}$$

α is the *variational parameter*, and varying it will span all Gaussian functions with a mean value 0. This way, we will see how the electron interaction pertubation maps to a harmonic oscillator potential of a variational frequency $\alpha\omega$.
The second trial wave function builds on the first one, adding another parameter β. We add another exponential term, this time taking the relative distance between the electron into account. Taking into account the repulsive interaction between the electron, we want the added term to have a minima where the distance between the electrons is 0 and a maxima as the electrons move away from each other. The second trial function looks like this:

$$\Psi_{T2} = Ce^{\alpha\omega(r_1+r_2)/2}e^{r_{12}/(2+2\beta r_{12})} \tag{16}$$

We will also need to apply our Hamilton operator (2) on these trial wave functions. To calculate the local energy, we will first need to find the Laplacian of the wave function of the i'th electron

$$\begin{aligned}\nabla_i^2\Psi_{T1} &= \frac{\partial^2\Psi_{T1}}{\partial r^2} + \frac{2}{r}\frac{\partial\Psi_{T1}}{\partial r_i} \\ &= \frac{\partial}{\partial r}\left(-\alpha\omega r_i\Psi_{T1}\right) + \frac{2}{r_i}(-\alpha\omega r_i)\Psi_{T1} \\ &= \Psi_{T1}\left(-\alpha\omega + \alpha^2\omega^2 r_i^2 - 2\alpha\omega\right) \\ &= \Psi_{T1}\left(\alpha^2\omega^2 r_i^2 - 3\alpha\omega\right)\end{aligned}$$

Using the Hamiltonian of the system from (1) without the Coulomb interaction, we get that the local energy from (11) becomes

$$\begin{aligned}E_{L1} &= -\frac{1}{2}\alpha^2\omega^2(r_1^2+r_2^2) + 3\alpha\omega + \frac{1}{2}\omega^2(r_1^2+r_2^2) \\ &= \frac{1}{2}\omega^2(r_1^2+r_2^2)(1-\alpha^2) + 3\alpha\omega\end{aligned} \tag{17}$$

Adding the Coulomb interaction simply adds a term:

$$E_{L1} = \frac{1}{2}\omega^2(r_1^2+r_2^2)(1-\alpha^2) + 3\alpha\omega + \frac{1}{r_{12}} \tag{18}$$

For the second trial wave function, the Laplacian of the i'th electron takes a bit more of a complicated form. Breaking it up, defining $\psi(r_{12}) = e^{r_{12}/(2+2\beta r_{12})}$ such that $\Psi_{T2} = \Psi_{T1}\phi$, the result of the Laplacian becomes:

$$\begin{aligned}\nabla_i^2\Psi_{T2} =& \phi\nabla_i^2\Psi_{T1} + \frac{\Psi_{T2}}{2(1+\beta r_{12})^2}\Bigg(-\alpha\omega r_{12} \\ &\cdot\left(x_i(x_i-x_j) + y_i(y_i-y_j) + z_i(z_i-z_j)\right) \\ &+ \frac{1}{2(1+\beta r_{12})^2} + \frac{2}{r_{12}} - \frac{2\beta}{1+\beta r_{12}}\Bigg)\end{aligned}$$

The local energy will simply have an added term compared to the local energy of the first trial function, (18), as

$$\begin{aligned}E_{L2} = E_{L1} + \frac{1}{2(1+\beta r_{12})^2}\Bigg(&\alpha\omega r_{12} \\ &- \frac{1}{2(1+\beta r_{12})^2} - \frac{2}{r_{12}} + \frac{2\beta}{1+\beta r_{12}}\Bigg)\end{aligned} \tag{19}$$

Finally, we will look at the *cusp condition* for these trial wave functions. The cusp condition entails that

[10] David J. Griffiths and Darrel F. Schroeter. *Introduction to Quantum Mechanics*. Third Ed. ISBN: 9781107189638.

the local energy of the wave functions does not contain any singularities, specifically when $r_{12} \to 0$. This is trivially fulfilled for E_{L1} when the Coulomb interaction is not accounted for, but when it is introduced, it breaks down. However, taking the limit as $r_{12} \to 0$ for the local energy of the second trial function, we get

$$\begin{aligned}\lim_{r_{12}\to 0} E_{L2} = \lim_{r_{12}\to 0} &\frac{1}{2}\omega^2\left(r_1^2 + r_2^2\right)\left(1-\alpha^2\right) \\ &+ 3\alpha\omega + \frac{1}{r_{12}} \\ &+ \frac{1}{2(1+\beta r_{12})}\left(\alpha\omega r_{12} - \frac{1}{2(1+\beta r_{12})}\right. \\ &\left. - \frac{2}{r_{12}} + \frac{2\beta}{1+\beta r_{12}}\right) \\ &= \frac{1}{2}\omega^2\left(r_1^2 + r_2^2\right)\left(1-\alpha^2\right) + 3\alpha\omega - \frac{1}{4} + \beta\end{aligned}$$

So the cusp condition as $r_{12} \to 0$ is fulfilled for Ψ_{T2}.

References

Collins, George. *The virial theorem in stellar astrophysics*. Tucson: Pachart Pub. House, 1978. ISBN: 9780912918136.

Foulkes, Matthew et al. "Quantum Monte Carlo simulation of solids". In: *Reviews of Modern Physics* 73 (Feb. 2001). DOI: 10.1103/RevModPhys.73.33.

Drummond, N., Mike Towler, and R. Needs. "Jastrow correlation factor for atoms, molecules, and solids". In: *Physical Review B* 70 (Feb. 2008). DOI: 10.1103/PhysRevB.70.235119.

Fevang, C. M. and H. Kvernmoen. "Implementation of the Jacobi eigenvalue method with classical and quantum mechanical applications". In: (Sept. 2020). URL: https://github.com/hkve/FYS3150/blob/master/Project2/report/Project2_final.pdf.

Hjemgaard, B, H. Kvernmoen, and C. M. Fevang. "Estimating the critical temperature of a ferromagnetic material using the 2D Ising model". In: (Nov. 2020). URL: https://github.com/hkve/FYS3150/blob/master/Project4/report/Project4.pdf.

Griffiths, David J. and Darrel F. Schroeter. *Introduction to Quantum Mechanics*. Third Ed. ISBN: 9781107189638.